The Magnetic and Mechanical Properties of Sintered Ceramic Magnets $Sr_xBa_{1-x}Fe_{12}O_{19}$

Toto Rusianto, M. Waziz Wildan, Kamsul Abraha, and Kusmono.

***Abstract*— The magnetic and mechanical properties of sintered ceramic magnets with composition $Sr_xBa_{1-x}Fe_{12}O_{19}$ with mole fraction ratio (x) have been investigated. The $Sr_xBa_{1-x}Fe_{12}O_{19}$ with mole fraction ratio to adjust with x = 0, 0.25, 0.5, 0.75, and 1 were calcined at temperature of 1100 °C. Subsequently, the calcined powder was compacted and sintered to form sintered pellets and bars. For determine of sintering temperature, mixture of hematite and barium carbonate was calcined at temperature 1100 °C, compacted, and then sintered at various temperature of 1000, 1100, and 1200 °C. The magnetic properties are determined by hysteresis curve that was established using VSM machine. X-ray diffraction was used to investigate crystal structure of the elements. The Archimedes principle was practiced to measure density of sintered products. The mechanical properties were examined using flexural strength and Vickers hardness. As a result of the research, increased of the fraction mole x would increase Ms of the $Sr_xBa_{1-x}Fe_{12}O_{19}$. At the x = 0 for $SrFe_{12}O_{19}$ and x = 1 for $BaFe_{12}O_{19}$ were the Ms of 41.14 emu/g and the Ms of 80.32 emu/g, respectively. Otherwise, increased of the mole fraction x would decreased Hc. The Hc of the $SrFe_{12}O_{19}$ more than the $BaFe_{12}O_{19}$ were of 3.64 kOe and 5.22 kOe, respectively. Whereas the BH max of 4.22 MGOe was highest of the x = 0.25 for the $Sr_{0.25}Ba_{0.75}Fe_{12}O_{19}$. The flexural strength and Vickers hardness did not change with increasing of the x mole fraction. However, the flexural strength and Vickers hardness increased with increasing sintering temperature.**

***Index Term*— Ceramic magnets, energy product, barium, strontium, hexaferrite.**

I. Introduction

The term ferrite is applied to attribute to all magnetic ceramic materials containing iron oxide as a primary component. The ferrites have given greatly as special component applications because of their magnetic and insulating properties at room temperature. The ferrites have spinels, garnets, and hexagonal structures. The ferrite with hexagonal structure named hexaferrite that have used for permanent magnet for long time. The hexaferrite has been a material of intensive study for several decades due to the experience that the compound has attractive of the permanent magnet market since shortly after its exploration in the 1950s [1]. The hexaferrites have much more essentials application for electric motors, speakers, microwave, and magnetic recording [2]. The hexaferrite structures was built up by stacking sequences of three basic blocks of crystalline structures S-block ($Me^{2+}Fe_4O_8$) where Me is divalent metal ion, R-block $((Ba,Sr)Fe_6O_{11})^{2-}$, and T-block $((Ba,Sr)_2Fe_8O_{14})$. The hexagonal ferrites structures can be classified into six types depending on their chemical formulas and stacking sequences M-type $(Ba,Sr)Fe_{12}O_{19}$, Y-type $(Ba,Sr)_2Me_2Fe_{12}O_{22}$, W-type $(Ba,Sr)Me_2Fe_{16}O_{27}$, Z-type $(Ba,Sr)_3Me_2Fe_{24}O_{41}$, X-type $(Ba,Sr)_2Me_2Fe_{28}O_{46}$, and U-type $(Ba,Sr)_4Me_2Fe_{36}O_{60}$) [3]. M-type has the plainest structure. Barium ferrite is one of type the hexagonal ferrite that called barium hexaferrite [4]. It has relatively high Curie temperature, high magnetic anisotropy field, high coercive force, excellent chemical stability and corrosion resistivity [5]. The most known hexaferrite is the M-type whose structure can be constructed up from the S blocks interposed by the R block and be symbolically described as RSR*S* (Fig. 1) [6]. The hexagonal ferrite of M-type is constructed by crystalline with 11 different symmetry sites for 64 ions per unit cell. Gorter's model give the magnetic structure of 24 Fe^{3+} atoms, which are arranged over five separate sites two tetrahedral sites and three octahedral sites. The five sites are tided through ferromagnetic super exchange interaction via O^{2-} ions [2].

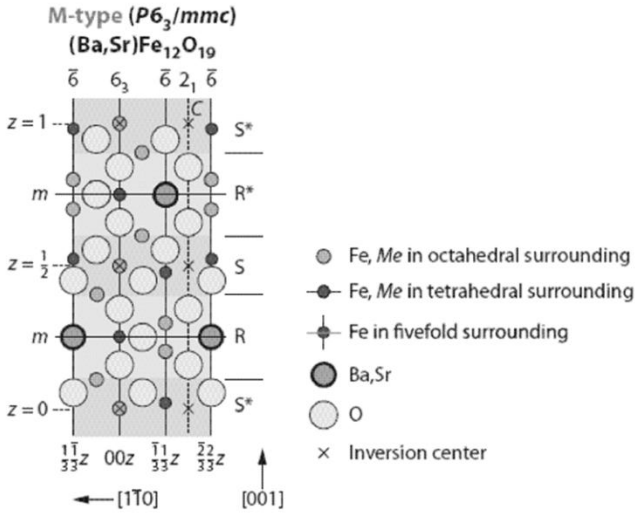

Fig. 1. Schematic hexaferrites crystal structures, the cross section views of the (110) plane M-type $(Ba,Sr)Fe_{12}O_{19}$ [6]

This work was supported by the Ministry of Education and Culture of The Republic of Indonesia, Directorate General of Higher Education, Kopertis Wilayah V Yogyakarta, under the Competitive Grant Program (Hibah Bersaing), contract number: 1331/K5/KM/2014.

Toto Rusianto is with the Department of Mechanical Engineering, Institute of Sciences & Technology Akprind Yogyakarta 55222 ID (e-mail: toto@akprind.ac.id and Postgraduate student of Department of Mechanical and Industrial Engineering, Gadjah Mada University Yogyakarta 55281 ID (e-mail: toto.rusianto@mail.um.ac.id).

M. Waziz Wildan is with the Department of Mechanical and Industrial Engineering, Gadjah Mada University Yogyakarta 55281 ID (e-mail: m_wildan@ugm.ac.id).

Kamsul Abraha is with the Department of Physics, Gadjah Mada University Yogyakarta 55281 ID (e-mail: kamsul@ugm.ac.id).

Kusmono is with the Department of Mechanical and Industrial Engineering, Gadjah Mada University Yogyakarta 55281 ID (e-mail: kusmono@ugm.ac.id).

The W-type hexagonal ferrites $BaMe_2Fe_{16}O_{27}$, (where Me stacks for any divalent element), have a crystalline structure built up as a superposition of S and R blocks, where the S block have the formula Fe_6O_8 and R block has the formula $BaFe_6O_{11}$. Y-hexaferrite ($Ba_2B_2Fe_{12}O_{22}$) structure in ionic substituted M-hexaferrite distribution of metallic ions between the discrete sub lattices is greatly changed by replacement of Br with Sr [7].

The Y-type hexagonal ferrites with composition $Ba_2Me_2Fe_{12}O_{22}$ (Me = Zn, Co, Mg, Mn, etc.) have a crystalline structure built up as a superposition of S and T block [8]. The Z-type ferrites (Ba, $Me_2Fe_2O_4$) present a more complex crystalline structure than that of M, Y and W compounds. The unit cell is built up by all the three basic structural blocks S, R and T and the divalent and trivalent metallic cations are distributed among ten different lattice sites [9]. The X-type systems are usually ticked as L_2M_2X where L stands for large ion and M for divalent ion. One formula unit of X-type is $L_2M_2Fe_{28}O_{46}$, one unit cell of X-type contains 3 stacking sequence of X-type is RSRSSR*S*R*S*S*. Space group of X structure is R3m [10]. The U-type hexaferrites formation with the general chemical formula $Ba_4B_2Fe_{36}O_{60}$, where B is Co, Ni, Zn was reported by several researcher. They reported, that the hexaferrites form a group of complex oxides in the system MO–Fe_2O_3–MeO, where M = Ba, Sr, Ca and Me = Mn, Fe, Co, Ni, Cu, Zn. Since this work is limited to the U-type hexaferrites, the term hexaferrites will refer to Ba-hexaferrites. U-hexaferrites are constructed from intermediate phases of Y-type hexaferrite ($Ba_2B_2Fe_{12}O_{22}$) and M-type hexaferrite ($BaFe_{12}O_{19}$) [11]. The ferrite materials have many important applications it's not only for magnetic materials, but also for application in modern telecommunication and electric device [12]. The permanent magnet materials Ba hexaferrites and Sr hexaferrites (BaM and SrM) have been synthesized through various techniques *i.e.* co-precipitation, including sol–gel synthesis, the use of organic precursors or glass ceramic, citrate nitrate synthesis and ceramic processing methods [7]. Milling process can introduce improvement materials into the mixture. Furthermore, Ba/SrM were made by a standard ceramic routed and sintered between 1100 to 1350 ^{O}C to give a high coercivity [13].

Conventional solid-state reactions for synthesis strontium and barium ferrite powders was obtained a high temperature calcinations of milled mixtures of hematite with strontium carbonate or and barium carbonate. The present research determined the optimal conditions for the solid-state synthesis $Sr_xBa_{1-x}Fe_{12}O_{19}$ as influence on the magnetic and mechanical properties of the resulting sintered product. The mechanical properties include three point bending, and Vickers hardness.

II. Methodology and Materials for Research

$Sr_xBa_{1-x}Fe_{12}O_{19}$ powder was prepared by conventional technique mixing hematite powder with strontium carbonate and barium carbonate in mole fraction ratio for five hours in alcohol. The mole fraction ratio of composition the powders was adjusted to x = 0, 0.25, 0.5, 0.75, and 1. The homogeneous mixtures were calcined at temperature of 1100 °C in a furnace with air atmosphere for two hours. The calcined specimens with binder polyvinyl alcohol (PVA) of 1% by weight were uniaxially compacted with a pressure of 30 MPa to produce bars and cylindrical green compacts. The specimen dimensions were length of 50 mm, width of 8 mm, and thickness of 8 mm for bar and diameter of 16 mm and thickness of 10 mm for cylinders, respectively. The green compacts were sintered at various temperature of 1000, 1100, and 1200 ^{O}C. Characterization of the magnetic properties of a small magnetic material samples were examined using vibrating sample magnetometer (VSM) with in an applied field magnetic between −10 kOe to +10 kOe. The result of magnetic characterization was presented in the form a hysteresis curve. Phases characterization were observed by Shimadzu XRD-6000 diffractometer with Cu-Kα radiation (λ=1.54056). The X-ray powder diffraction (XRD) patterns of specimens treated in a wide range of 2θ from 20^{O} to 70^{O} with a scan speed of 5.00^{O}/min and sampling pitch of 0.02^{O}. The patterns of XRD were matched using a JCPDS standard. The density of the specimens was determined using Archimedes principle method. Mechanical properties of the sintered specimens were examined, with i.e. flexural strength and Vickers hardness testing.

III. Results and Discussion

A. XRD analysis.

The mixture of $BaCO_3$ and $SrCO_3$ with various x mole fraction and the Fe_2O_3 were calcined to form $Sr_xBa_{1-x}Fe_{12}O_{19}$. The XRD patterns of the $Sr_xBa_{1-x}Fe_{12}O_{19}$ specimens are shown in Fig. 2. The XRD patterns in Fig. 2(a) and 2(e) indicate of $BaFe_{12}O_{19}$ and $SrFe_{12}O_{19}$ phases, respectively. The phase exhibit peaks of 2 theta at 32.22^{O} (I/I_0 = 100%) and 34.16^{O} (I/I_0 = 98%) with d-spacing of 2.777 Å and 2.6239 Å for $BaFe_{12}O_{19}$, respectively. While, for the $SrFe_{12}O_{19}$ phase exhibit peaks 2 theta at 32.28^{O} (I/I_0 = 95%) and 34.22^{O} (I/I_0 = 100%) with d-spacing of 2.772 Å and 2.6194 Å, respectively. The index crystal (h k l) of the phases have the same index of (1 0 7) and (1 1 4). D-spacing of $SrFe_{12}O_{19}$ are lower than d-spacing of $BaFe_{12}O_{19}$. It corresponds with diameter of Sr^{2+} ion of 1.27 Å less than diameter of Ba^{2+} ion of 1.43 Å.

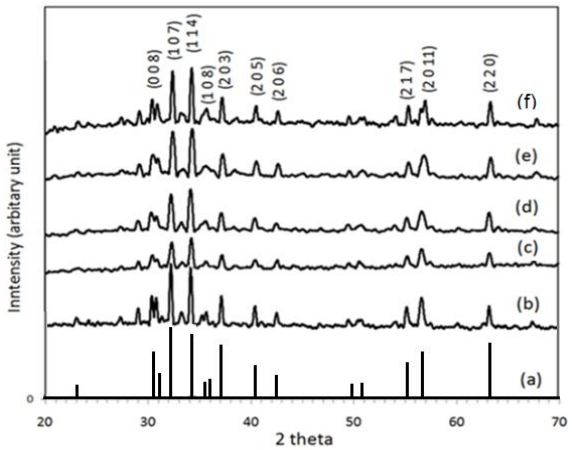

Fig. 2. The XRD patterns of the $Sr_xBa_{1-x}Fe_{12}O_{19}$ with various molar ratio (a) JCPDS 27-1029 for barium hexaferrite (b) $BaFe_{12}O_{19}$, (c) $Sr_{0,25}Ba_{0,75}Fe_{12}O_{19}$, (d) $Sr_{0,5}Ba_{0,5}Fe_{12}O_{19}$, (e) $Sr_{0,75}Ba_{0,25}Fe_{12}O_{19}$ and (f) $SrFe_{12}O_{19}$

The BaM has lattice constants with the parameters c = 23.17 Å and a = 5.89 Å. While, the lattice parameters of SrM are 23.03 Å for the c-axis length and 5.86 Å for a-axis [13]. The typical XRD pattern shows as according to JCPDS number 27-1029 for barium hexaferrite and JCPDS number 024-1207 for Strontium hexaferrite.

B. Density

Fig. 3 shows the relative densities of the specimens with the mole fraction of the $Sr_xBa_{1-x}Fe_{12}O_{19}$. The molecular mass of BaM and SrM of 1112 g/mole and 1062 g/mole with theoretical density of 5.295 gr/cm^3 and 5.101 g/cm^3, respectively [13]. The bulk density BaM and SrM of 4.73 gr/cm^3 and 4.68 gr/cm^3 with relative density of 89 % and of 91 % respectively, at sintering temperature of 1200 ^{O}C, although in fact the ceramic materials frequently has a density as low as 90% of theoretical density. The relative density of the specimens do not change with increase of mole fraction x. Combined of the mole fraction x has a density between density of BaM and SrM. Many sintering ceramic magnets aids involve either the formation of relatively low temperature with glassy phases (e.g. SiO_2, B_2O_3, Bi_2O_3) added to increase density [13]. The low density can be increased by enhancing the sintering temperature. However, the high sintering temperature ≥ 1200 ºC result in the formation of coarse grain [14]. The grain size of the BaM and SrM phases can grow larger. The larger grain size of the magnetic materials would decrease the magnetic properties than smaller grain size. With the reason, the sintering temperature was limited until temperature of 1200 ºC.

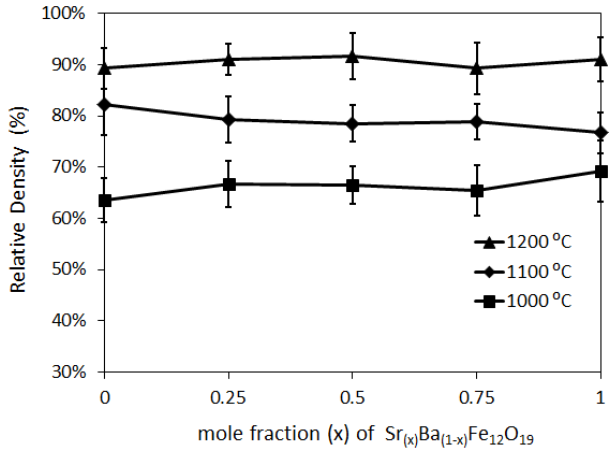

Fig. 3. Effect of sintering temperatures to relative densities of the $Sr_xBa_{1-x}Fe_{12}O_{19}$ with mole fraction ratio (x).

C. Magnetic Properties

Fig. 4 shows hysteresis curve of $BaFe_{12}O_{19}$ with vatious sintering temperature. The curve have a wide coercivity that indicate a ferromagnetic property. The magnetic properties of the specimens have compiled in Table 1. From Table 1 the magnetic properties (Ms, Mr and Hc) of the specimens were highest at sintering temperature 1200 ^{O}C, otherwise the energy product maximum of the sample was higgest of 4.07 MGOe at sintering temperature 1100 ^{O}C.

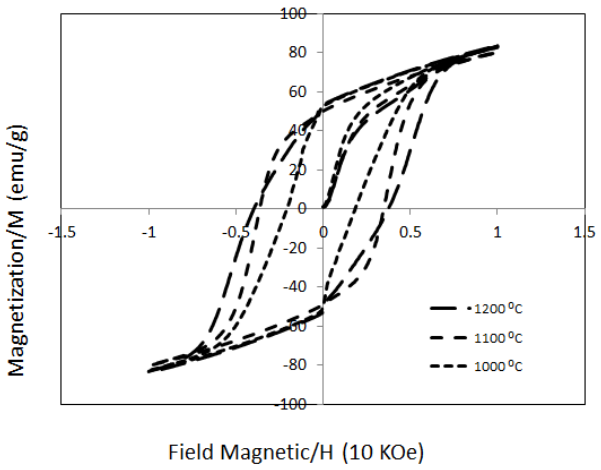

Fig. 4. Hysteresis curves of the $BaFe_{12}O_{19}$ with various of sintering temperature.

TABLE I
EFFECT SINTERING TEMPERATURE TO MAGNETIC PROPERTIES OF THE $BaFe_{12}O_{19}$

Magnetic properties	Sintering Temperature		
	1000 ^{O}C	1100 ^{O}C	1200 ^{O}C
Ms (emu/g)	82.82	80.32	83.60
Mr (emu/g)	52.67	50.08	53.38
Mr/Ms	0.64	0.62	0.64
Hc (kOe)	2.06	3.64	3.94
BH max (MGOe)	1.38	4.07	3.38

The highest BH max at a the sintering temperature 1100 ^{O}C is advantage for application of permanent magnet for electric generator or electric motor. Ms, Mr and Hc of the specimens were highest at sintering temperature 1200 ^{O}C, but in the fact the energy product as an indicator of quality of permanent magnet. Therefore, The sintering temperature 1100 ^{O}C used as a route of the research. The decreasing of BH max at higher temperature may be a consequence of bigger grain size formed as a result of their merger with each other. It is well known that grain size has a significant effect on the magnetic properties of the magnetic materials. When the grains size are smaller than the critical single domain size, the grains size are mainly in single domain. On the reverse, when the grain size becomes bigger than the critical value most of them would exist in multi domain. With an increase in the sintering temperature the grain size also increases towards the critical single domain size [14].

Fig. 5 presents hysteresis curve of $Sr_xBa_{1-x}Fe_{12}O_{19}$ where mole fraction of x = 0 for $SrFe_{12}O_{19}$ have a wide of hysteresis curve than of x = 1 for $BaFe_{12}O_{19}$. The $SrFe_{12}O_{19}$ have higher Hc of 5.22 kOe than $BaFe_{12}O_{19}$ with Hc of 3.64 kOe. Otherwise, the $SrFe_{12}O_{19}$ has a lower Ms of 41.14 emu/g than the $BaFe_{12}O_{19}$ with Ms of 80.32 emu/g. It can be seen at Table 2. The ceramic magnet that was reported in this paper has satisfied magnetic properties for application required. The coercivity of SrM have slightly higher values than of BaM. The SrM has Bohr magnetons of 20.6 µB and giving a very high magnetic anisotropy field of 20 kOe in the c-axis. Compare with BaM that has Bohr magnetons 20 µB and magnetic anisotropy field of 17 kOe along the c-axis [12]. The ratio of remanence

magnetization and saturation magnetization Mr/MS was more than 0.5, it indicated the $Sr_xBa_{1-x}Fe_{12}O_{19}$ of randomly oriented multi domain particles [15]. Mr/Ms is found to be around of 0.5 that expected value for randomly packed single-domain particles having the shape of magnetic anisotropy [5].

The two most important characteristics relative to applications for magnetic materials are the coercivity and energy product designated as BH max. The energy product corresponds to the area of the largest BH rectangle that can be constructed within the second quadrant of the hysteresis curve. In this paper present the maximum B×H at mole fraction x = 0.25 of $Sr_{0.25}Ba_{0.75}Fe_{12}O_{19}$, and the calculated of energy product result the BHmax of 4.22 MGOe. The value of the energy product is representative of the energy required to demagnetize a permanent magnet.

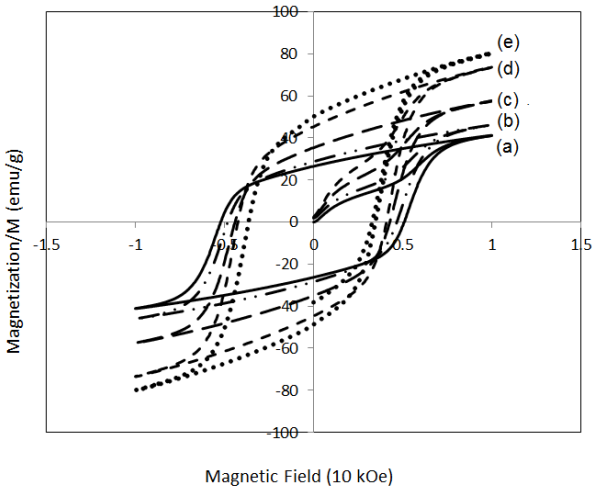

Fig. 5. Hysteresis curves of the (a) $SrFe_{12}O_{19}$, (b) $Sr_{0.75}Ba_{0.25}Fe_{12}O_{19}$, (c) $Sr_{0.5}Ba_{0.5}Fe_{12}O_{19}$ (d) $Sr_{0.25}Ba_{0.75}Fe_{12}O_{19}$, and (e) $BaFe_{12}O_{19}$ at temperature sinter 1100 ^{O}C.

TABLE 2: MAGNETIC PROPERTIES OF $Sr_xBa_{1-x}FE_{12}O_{19}$ WITH VARIOUS MOLE FRACTIONS x

Magnetic properties	mole fractions (x) of $Sr_xBa_{1-x}Fe_{12}O_{19}$				
	0.00	0.25	0.50	0.75	1.00
Ms (emu/g)	80.32	73.66	57.69	46.23	41.14
Mr (emu/g)	50.08	45.22	35.29	28.67	26.46
Mr/Ms	0.62	0.61	0.61	0.62	0.64
Hc (kOe)	3.64	4.24	4.41	4.81	5.22
BH max (MGOe)	4.07	4.22	3.28	2.93	2.90

D. Mechanical Properties

Fig. 6 shows the variation of flexural strength of sintered specimens as a function of mole fractions x and sintering temperatures. The flexural strength increased with increasing the sintering temperatures. Fig. 7 shows the Vickers hardness of specimens with various sintering temperature. The hardness characterization have a same phenomenon with flexural strength, the which the hardness increases with increasing the sintering temperature. The sintering temperature has enhanced density of specimens that cause the porosity decreased. The porosity is a source of initial crack that decrease strength of a material. Thus, the decreased porosity would increase of strength of a material. All the specimens at a sintering temperature 1000 ^{O}C have low flexural strength and low hardness. Sintering process has three stages, Initial stage in sintering process particles has surface contact, neck formation at the contact point, and the green body is generally lacking in solidification. It was caused the specimens have low density and low strength. Intermediate stage of sintering occur neck growth of point contact particles. A dense polycrystalline solid is usually obtained in final stage of sintering process at higher sintering temperature than initial stage sintering. However, in sintering can result only locally contact at interface of particles.

In such a indication a change of the shape and the size of the pores and the particles are commonly defined as grain growth or coarsening. In ceramic materials the final sintering stage starts at about 93% to 95% of theoretical density, when porosity is decreased and already isolated. At last, at the end of final sintering stage, porosity can be eliminated and the strength of materials increased.

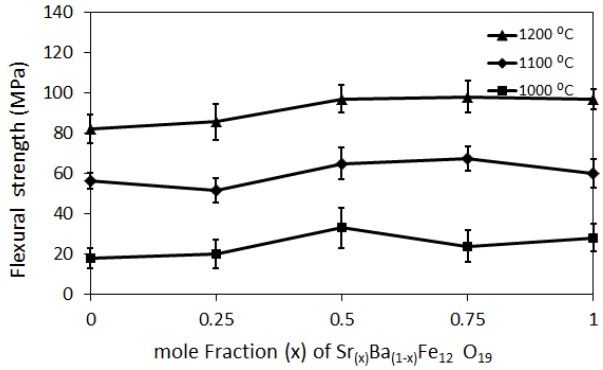

Fig. 6. The effect of mole fraction x and various sintering temperature on flexural strength

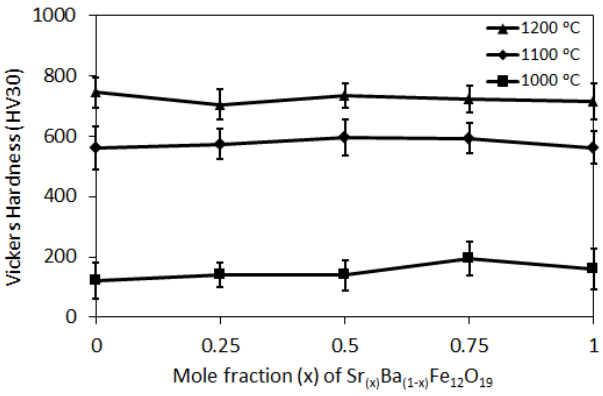

Fig. 7. The effect of mole fraction x and various sintering temperature on Vickers hardness

IV. CONCLUSION

The sintered ceramic magnets $Sr_xBa_{1-x}Fe_{12}O_{19}$ with various of mole fraction x were successfully synthesized with conventional method. At sintering temperature 1100 ^{O}C the Ms and the Mr decreased with increased x mole fraction, while the Hc increased. The highest of BH max occurred at mole fraction x = 0.25 for $Sr_{0.25}Ba_{0.75}Fe_{12}O_{19}$. The flexural strength and the Vickers hardness increase with increasing sintering temperature.

REFERENCES

[1] C.M. Fang., F. Kools., R.Metselaar, G de With, and R.A.de Goot, "Magnetic and electric properties of strontium hexaferrite ($SrFe_{12}O_{19}$) from first principles calculations" Journal of physics: condensed matter, vol. 15 pp.6229-6237, August 2003.

[2] K. Samikannu, J. Sinnappan, S. Mannarswamy, T. Cinnasmy, K. Thirunavukarasu, "Synthesis and magnetic properties of conventional and microwave calcined strontium hexaferrite powder" Materials Sciences and Application, vol. 2 pp. 638-642, June 2011

[3] K. Okumura, T. Ishikura, M. Soda, T. Asaka, H. Nakamura, *et.al*., "Magnetism and magnetoelectricity of a U-type hexaferrite $Sr_4Co_2Fe_{36}O_{60}$," Applied Physics Letters, vol. 98, 21250 pp.1-3, 2011.

[4] I. Ştefan, , R. Chiriac, C. Nicolicescu, and M. Ciobanu, "Research on synthesis of barium hexaferrite powders processed by mechanical alloying," J. Optoelectronics and Advanced Materials, vo. 13 883-886. July 2011.

[5] M.M. Rashad and I.A. Ibrahim, "Improvement of the magnetic properties of barium hexaferrite nanopowders using modified co-precipitation method" Journal Materials Sciences, Material Electronics, vol. 22 pp. 1796-1803, 2011.

[6] T. Kimura, "Magnetoelectric hexaferrites," The Annual Review of Condensed Matter Physics is Phys, vol. 3, pp 93-110, December 2011.

[7] A. A. Nourbakhsh, M. Nourbakhsh, M. Shaygan, and K. J. D. Mackenzie, "The effect of nano sized $SrFe_{12}O_{19}$ additions on the magnetic properties of chromium-doped strontium-hexaferrite ceramics," J Mater Sci: Mater Electron vol. 12, pp.1297–1302, February 2011.

[8] Y. Bai, F. Xu, L. Qiao, and Ji Zhou, "Effect of Mn doping on physical properties of Y type hexaferrite" Journal of Alloys and Compounds, vol. 473, pp. 505-508. 2009.

[9] T. Nakamura, and E. Hankui, "Control of high-frequency permeability in polycrystalline (Ba,Co)-Z-type hexagonal ferrite," Journal of Magnetism and Magnetic Materials, vol. 257, pp. 158–164. 2003.

[10] K. Kouril, "Local structure of hexagonal ferrites studied by NMR" Doctoral Thesis, Dept. of Low Temperature Physics, Faculty of Mathematics and Physics, Charles University in Prague, 2013.

[11] D. Lisjak, P. Mc Guiness , and M. Drofenik, "thermal instability of co-substituted barium hexaferrites with U-type structure," J. Mater. Res., vol. 21, pp. 420-427, February 2006.

[12] Sasito, E., B. Soegijono, A, Manaf, "Thermo electric power study of CuZn Ferrite in magnetic transition phase as yield of flow injection synthesis co-precipitation reaction" , International Journal of Basic & Applied Sciences IJBAS-IJENS vol. 13 no. 05, October 2013.

[13] R. C. Pullar, "Hexagonal ferrites: A review of the synthesis, properties and applications of hexaferrite ceramics," Progress in Materials Sciences vol. 57, pp. 1191-1334, 2012.

[14] M. Ahmad, I. Ali, F. Aen, M.U. Islam, M. N. Ashiq, S. Atiq, W. Ahmad, and M.U, Rana, "Effect of sintering temperatura on magnetic and electricals properties of nano size Co_2W hexaferrite" Journal Ceramic international vol. 38 pp. 1267-1273, 2012.

[15] D. Bahadur, S. Rajakumar, And A. Kumar, "Influence of fuel ratios on auto combustion synthesis of barium ferrite nano particles," J. Chem. Sci., Vol. 118, pp. 15–21, January 2006.